



## Flooding on California's Russian River: Role of atmospheric rivers

F. Martin Ralph,<sup>1</sup> Paul J. Neiman,<sup>1</sup> Gary A. Wick,<sup>1</sup> Seth I. Gutman,<sup>1</sup>  
Michael D. Dettinger,<sup>2</sup> Daniel R. Cayan,<sup>2</sup> and Allen B. White<sup>3</sup>

Received 24 April 2006; revised 12 May 2006; accepted 23 May 2006; published 1 July 2006.

[1] Experimental observations collected during meteorological field studies conducted by the National Oceanic and Atmospheric Administration near the Russian River of coastal northern California are combined with SSM/I satellite observations offshore to examine the role of landfalling atmospheric rivers in the creation of flooding. While recent studies have documented the characteristics and importance of narrow regions of strong meridional water vapor transport over the eastern Pacific Ocean (recently referred to as atmospheric rivers), this study describes their impact when they strike the U.S. West Coast. A detailed case study is presented, along with an assessment of all 7 floods on the Russian River since the experimental data were first available in October 1997. In all 7 floods, atmospheric river conditions were present and caused heavy rainfall through orographic precipitation. Not only do atmospheric rivers play a crucial role in the global water budget, they can also lead to heavy coastal rainfall and flooding, and thus represent a key phenomenon linking weather and climate. **Citation:** Ralph, F. M., P. J. Neiman, G. A. Wick, S. I. Gutman, M. D. Dettinger, D. R. Cayan, and A. B. White (2006), Flooding on California's Russian River: Role of atmospheric rivers, *Geophys. Res. Lett.*, 33, L13801, doi:10.1029/2006GL026689.

### 1. Introduction

[2] It has long been known that the atmosphere accomplishes most of its midlatitude horizontal water vapor transport in narrow, elongated regions located within the warm sector of extratropical cyclones [e.g., *Browning and Pardoe*, 1973]. These regions are characterized by warm air temperatures, large water vapor content, and strong winds at low altitudes. Only recently, however, have the narrowness and importance of these features been adequately quantified. *Zhu and Newell* [1998] used a global numerical model to diagnose that >90% of the total meridional water vapor transport in the midlatitudes takes place in narrow corridors that constitute <10% of the Earth's circumference at mid-latitudes. These characteristics led to the term "atmospheric river." More recently, observational studies [*Ralph et al.*, 2004, 2005] used research aircraft and satellite observations over the eastern Pacific Ocean to quantify the horizontal and vertical structure of atmospheric rivers, as well as their synoptic environment and interannual variability. *Bao et al.*

[2006] then used a mesoscale numerical model to study the possible tropical origins of water vapor in several major West Coast storms. These types of storms are sometimes referred to as "Pineapple Express" events [*Higgins et al.*, 2000].

[3] While it is generally known that when storms move inland across the West Coast of the U.S. they can yield heavy rainfall and flooding, the contribution of atmospheric rivers to the heavy rain and flooding has not been fully documented. The atmospheric river concept provides a new and objective framework in which to examine and quantify atmospheric conditions related to rainfall intensity. This concept can help distinguish landfalling storms that generate heavy rainfall from those likely to produce lighter rain. This study uses experimental meteorological measurements from field studies near the Russian River of northern California (Figure 1) and Special Sensor Microwave Imager (SSM/I [*Hollinger et al.*, 1990]) polar-orbiting satellite observations of vertically integrated water vapor (IWV) since 1997 to examine the connection between atmospheric rivers and flooding on the Russian River (12-hourly composites of IWV data from several satellites were used to provide adequate spatial coverage). First, a focused case study of the flood-producing storm on 16–18 February 2004 is presented. Second, all floods on the Russian River between 1 October 1997 and 28 February 2006, i.e., the period when SSM/I data and experimental meteorological measurements are available, are examined for evidence of atmospheric river conditions.

### 2. Data

[4] To determine if atmospheric river conditions were present in the case study and the other flooding events, it was necessary to observe the spatial distribution of IWV offshore based on the approach developed in *Ralph et al.* [2004] using SSM/I data. Although the SSM/I IWV data alone cannot quantify moisture transport due to the lack of wind information, *Ralph et al.* [2004, 2005] showed that the SSM/I IWV data can be used as a proxy for detecting the presence of atmospheric rivers when the spatial distribution of IWV meets several criteria. In addition to using the SSM/I data, it was also necessary to determine if a threshold of 2 cm of IWV was exceeded with surface-based observations at the coast during each event, and if each event was characterized by strong low-level onshore winds with low-level jet (LLJ) structure. These are key characteristics of atmospheric rivers that make them regions of strong water-vapor transport. It should be noted that in atmospheric rivers over the eastern Pacific, 75% of the water vapor transport below 500 mb takes place within the lowest 2.25 km and occurs with LLJ wind structure [*Ralph et al.*, 2005].

<sup>1</sup>NOAA/Earth System Research Laboratory, Boulder, Colorado, USA.

<sup>2</sup>U.S. Geological Survey, Scripps Institution of Oceanography, La Jolla, California, USA.

<sup>3</sup>Cooperative Institute for Research in the Environmental Sciences/NOAA/ESRL, Boulder, Colorado, USA.

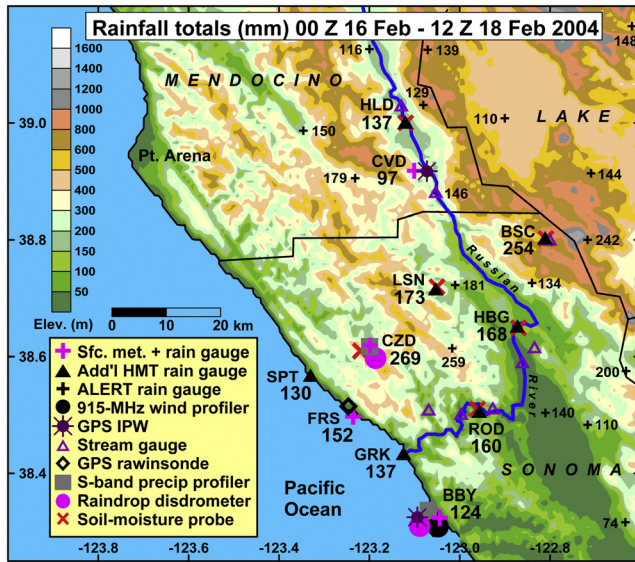


**Figure 1.** Terrain base map of northern California's Russian River watershed showing the locations of the observing systems (see key). The three-letter station names are given for the experimental sites. The numerical values represent the 60-h accumulated rainfall between 0000 UTC 16 February and 1200 UTC 18 February 2004.

[5] The wind information needed to diagnose the possible presence of an atmospheric river at the coast is provided by a 915-MHz wind profiler at Bodega Bay (BBY; Figure 1), which has been deployed by NOAA during most winters since 1997. This radar measures the hourly averaged vertical profile of the horizontal wind with 100 m vertical resolution from 100 m to 2–4 km above ground, with 1 m s<sup>-1</sup> wind speed accuracy [Carter et al., 1995]. Neiman et al. [2002] used profilers to determine that the hourly rainrate at coastal mountain sites was best correlated with the upslope component of the wind at 1 km above mean sea level (MSL), where

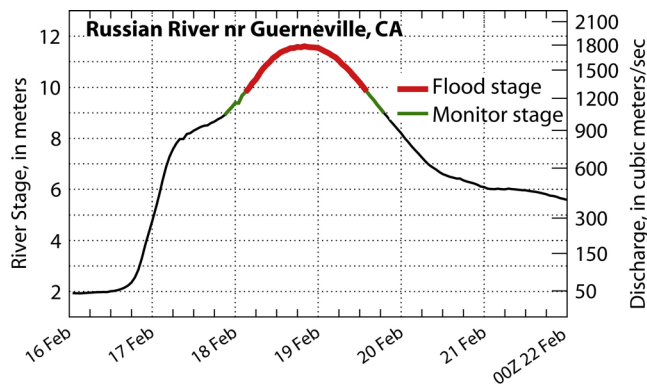


**Figure 2.** Hydrograph (river stage in meters; discharge in m<sup>3</sup> s<sup>-1</sup>) from the Russian River at Guerneville, CA (location marked by a triangle just west of ROD in Figure 1) between 0000 UTC 16 February and 0000 UTC 22 February 2004. The river stages are official National Weather Service designations.

roughly half of the hourly variability of rainrate is explained by hourly variability in upslope wind speed.

[6] While it would be ideal also to continuously observe the full vertical profile of water vapor transport, the technology to remotely monitor water vapor profiles is very costly, as is the alternative of launching radiosondes. Ralph et al. [2004] established the value of using SSM/I satellite-observed IWV as a proxy for atmospheric river detection offshore. The analogous approach at the coast uses surface-based GPS IWV retrievals at 0.5-h intervals with ~1 mm accuracy [Wolfe and Gutman, 2000]. One of these systems was first deployed at BBY in 2001, and additional sites in California were used as well. Several tipping-bucket rain gauges were sited along the coast and in the coastal mountains to provide better information on the spatiotemporal distribution of rainfall during the 2004 field season (Figure 1). Locations of additional observing systems critical to the diagnosis of the case study, including U.S. Geological Survey stream gauges, are shown in Figure 1.

### 3. Case Study

[7] A storm that struck northern California on 16–18 February 2004 produced >250 mm of rain in 60 h in the coastal mountains and ~100–175 mm elsewhere in the domain shown in Figure 1. This created heavy runoff on the Russian River, which exceeded flood stage at Guerneville on 18–19 February (Figure 2). The synoptic conditions at 1200 UTC 16 Feb included a strong (961 mb) extratropical cyclone located west of Washington, as well as a surface front arcing southeastward toward Oregon and then southwestward offshore of California. Rain began over the coastal mountains of the Russian River watershed at 0700 UTC 16 February as a warm front descended (Figures 3 and 4). The onset of rain also coincided with the development at BBY of orographically favored low-level upslope flow and an increase in IWV (Figures 3 and 4). After the warm front reached the surface at

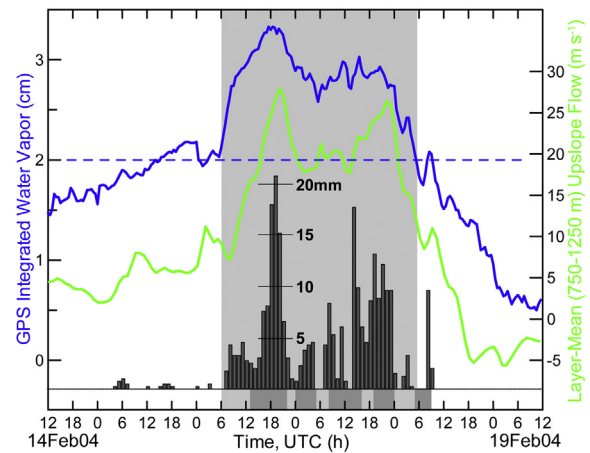


**Figure 3.** Time series of IWV (cm; blue) and layer-mean (750–1250 m MSL) upslope flow (m s<sup>-1</sup>; green) at BBY, and histogram of hourly rainfall (mm; see scale) at CZD, between 14–19 February 2004. The light gray-shaded bar marks atmospheric river conditions (IWV > ~2 cm; dashed blue line). The dark gray-shaded bars at the bottom denote LLJ episodes, as in Figure 4.

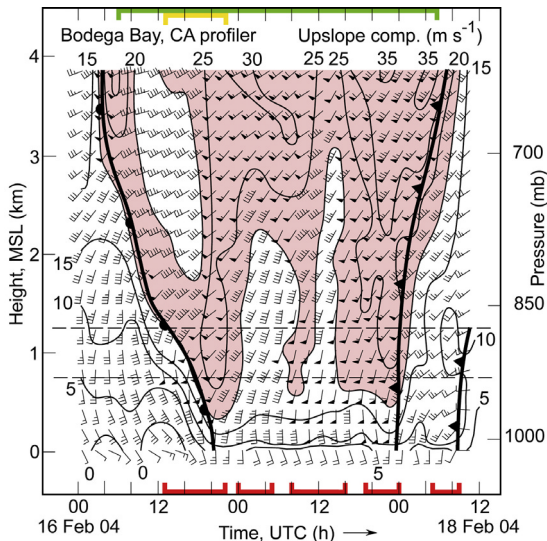


**Figure 4.** Time-height section of hourly averaged wind profiles, upslope-component isotachs ( $\text{m s}^{-1}$ , directed from  $230^\circ$ ;  $>20 \text{ m s}^{-1}$  red-shaded), and fronts at BBY on 16–18 February 2004 (wind flags =  $25 \text{ m s}^{-1}$ , barbs =  $5 \text{ m s}^{-1}$ , half-barbs =  $2.5 \text{ m s}^{-1}$ ). Colored brackets denote the following observations at BBY: red = LLJ episodes; green = IWB  $> 2 \text{ cm}$ ; yellow = IWB  $> 3 \text{ cm}$ . Data within the pair of dashed lines (750–1250 m MSL) were layer-averaged and presented in Figure 3.

2000 UTC 16 February, warm-sector conditions prevailed at the surface for 28 h (Figure 4). Finally, at 0000 UTC 18 February, the primary surface cold front crossed the watershed, and precipitation and IWB decreased greatly (Figures 3 and 4).

[8] Not only do the wind profiler data clearly establish that the event occurred within the warm sector of the storm, the data also establish that 27 of 35 hourly wind profiles in the warm sector at 1.25 km MSL had LLJ characteristics (i.e., wind speed maximum below 1.5 km that is  $\geq 2 \text{ m s}^{-1}$  larger than a local minimum aloft) centered at a mean altitude of 878 m MSL. The orographic nature of the rainfall in this event is shown in Figure 3, and is confirmed through correlation analyses (as in *Neiman et al.*, 2002; not shown), which reveal a correlation of 0.70 between the hourly, layer-averaged upslope wind speed at 750–1250 m MSL and hourly rainrate in the downstream mountains at Cazadero (CZD; Figure 1). In short, the Russian River watershed was exposed to the strong, moist onshore flow within the warm sector ahead of the primary cold front, i.e., the type of conditions that *Ralph et al.* [2003] and *Andrews et al.* [2004] showed as having contributed to the record-breaking flood on Pescadero Creek in the Santa Cruz Mountains in 1998. While 70% of the hourly variance of rain rate in the coastal mountains is explained due to hourly variations in upslope wind speed, it is also apparent that frontally forced vertical circulations associated with the warm and cold fronts also contributed to the largest rain rates (Figures 3 and 4), and thus also to the flooding (as was also seen in the Pescadero Creek flood analysis of *Ralph et al.* [2003]).

[9] Furthermore, reference to the IWB observations from the GPS receiver at BBY in this event (Figure 3) reveals that

IWB increased to well over 2.0 cm at the same time that significant rain began, and then decreased to well below 2.0 cm as the rain ended in the nearby mountains. During this  $\sim 48 \text{ h}$  period, when IWB continuously exceeded 2.0 cm, the local mountains received 273.6 mm of rain, or 94% of the 5-day total. This IWB-rainfall relationship supports the long-held concept that heavy rainfall occurs most readily in an environment with large IWB [*Weaver*, 1962]. It is also noteworthy that there were two periods of enhanced upslope winds near 1 km MSL, and that these corresponded to the periods of greatest IWB and greatest rainfall at CZD (Figure 3).

[10] Finally, SSM/I satellite-observed IWB data offshore on 16 February 2004 (Figure 5) reveal a narrow corridor of IWB  $> 2 \text{ cm}$  that is  $<1000 \text{ km}$  wide and  $>2000 \text{ km}$  long – characteristic of an atmospheric river [*Ralph et al.*, 2004]. This IWB plume stretches southwestward from the Russian River area and includes regions offshore of IWB  $> 3.0 \text{ cm}$ . Significantly, the general area where this region intersects the coast is where many streams on 17 February were characterized by daily flows within the top 0.2% of those observed historically (i.e.,  $\geq 30$  years of observations) for that date (Figure 5). The Russian River's Guerneville daily discharge on 18 February ranked 35th among 24,230 days on record (0.144 percentile) or second among 67 February 18s on record.

#### 4. All Floods Since 1997

[11] To further explore the relationship between atmospheric rivers and flooding on the Russian River, the approach taken in the detailed case study described above

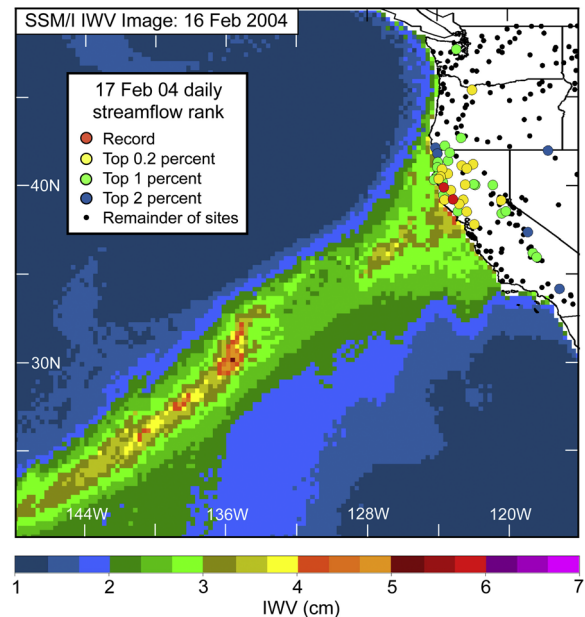


**Figure 5.** Composite SSM/I satellite image of IWB (cm; color bar at bottom) constructed from polar-orbiting swaths between  $\sim 1400$  and 1830 UTC 16 February 2004, and ranking of daily streamflows (percent; see inset key) on 17 February 2004 for those gauges that have recorded data for  $\geq 30$  years. The streamflow data are based on local time (add 8 h to convert to UTC).

**Table 1.** Daily Mean Flood- and Monitor-Stage Events ( $\geq 1275$  and  $1075 \text{ m}^3 \text{ s}^{-1}$ , respectively) on California's Russian River at Guerneville Between 1 October 1997 and 28 February 2006<sup>a</sup>

Event Rank Since 1 October 1997	Date of Peak Stage and Mean Flow, mm/dd/yyyy <sup>b</sup>	Days in Event	Peak Daily Mean Flow, $\text{m}^3 \text{ s}^{-1}$	Max. Hourly Stage, <sup>c</sup> m	Flood or Monitor Stage for Daily Mean	Atmos. River Structure in SSM/I <sup>d</sup>	GPS IWV > 2 cm? (Max IWV, cm)	BBY Profiler LLJ? (Max. Speed; $\text{m s}^{-1}$ )
1	01/01/2006	3	2320	13.4	Flood	Yes	Yes (3.4)	Yes (30)
2	02/18/2004	2	1700	11.6	Flood	Yes	Yes (3.3)	Yes (30)
3	02/07/1998	3	1460	11.4	Flood	Yes	NA	Yes (26)
4	02/03/1998	2	1350	11.8	Flood	Yes	NA	Yes (32)
5	12/16/2002	2	1240	11.1	Monitor	Yes	Yes (2.5)	Yes (30)
6	02/20/1998	1	1130	10.7	Monitor	No <sup>e</sup>	NA	Yes (22)
7	12/29/2005	1	1110	9.8	Monitor	Yes	Yes (3.6)	Yes (20)

<sup>a</sup>An event's duration is determined by the number of consecutive days for which the daily mean discharge exceeded monitor stage.

<sup>b</sup>The dates are Pacific Standard Time. To convert to UTC coordinates, add 8 h.

<sup>c</sup>Monitor stage is  $8.84 \text{ m}$  ( $\sim 1075 \text{ m}^3 \text{ s}^{-1}$ ); flood stage is  $9.75 \text{ m}$  ( $1275 \text{ m}^3 \text{ s}^{-1}$ ).

<sup>d</sup>An event is considered a landfalling atmospheric river in SSM/I satellite IWV data if it showed atmospheric river structure [see *Ralph et al.*, 2004] reaching the California coast within two days prior to the day of maximum stage for that event.

<sup>e</sup>This case had  $>2 \text{ cm}$  in SSM/I with appropriate structure, but 2 cm areas were not continuous, so it did not strictly meet atmospheric river criteria.

was repeated for all flood events for which the daily mean discharge exceeded the flow that corresponds to the monitor stage at Guerneville on the Russian River. The period of record used corresponds to the period when the SSM/I IWV observations and the BBY wind profiler data are available, i.e., since 1 October 1997 (GPS IWV data at BBY were not available for every event).

[12] A search of the daily mean streamflow records identified 14 dates between 1 October 1997 and 28 February 2006 when the "monitor-stage" flood threshold of  $8.84 \text{ m}$  or  $1075 \text{ m}^3 \text{ s}^{-1}$  was exceeded. A number of these dates were consecutive, and thus were grouped into "events" of 2 or 3 day duration. A total of 7 events were identified (Table 1). The criteria used to identify atmospheric river conditions were then applied to each day from 2 days before the date of maximum flow, up to that date. Table 1 shows

that all seven flooding events on the Russian River since 1 October 1997 correspond to conditions now generally recognizable as those of atmospheric rivers.

[13] The regional extent of the high streamflow (Figure 6a) was examined by determining how many times daily discharge at nearby stream gauges with  $\geq 30 \text{ y}$  of record exceeded the local 0.8-percentile on these 7 dates (discharge levels infrequent enough to suggest possible over-bank flooding at most sites). Sixteen gauges along 500 km of coastal California exceeded this threshold during 4 or more of the 7 flood events on the Russian River. A similar spatial pattern of large precipitation anomalies (averaged over the 7 events) is also associated with the events (Figure 6b). Finally, the entire domain shown in Figure 6 is also characterized in these events by  $5\text{--}10^\circ\text{C}$  anomalously warm minimum daily surface temperatures (not shown).

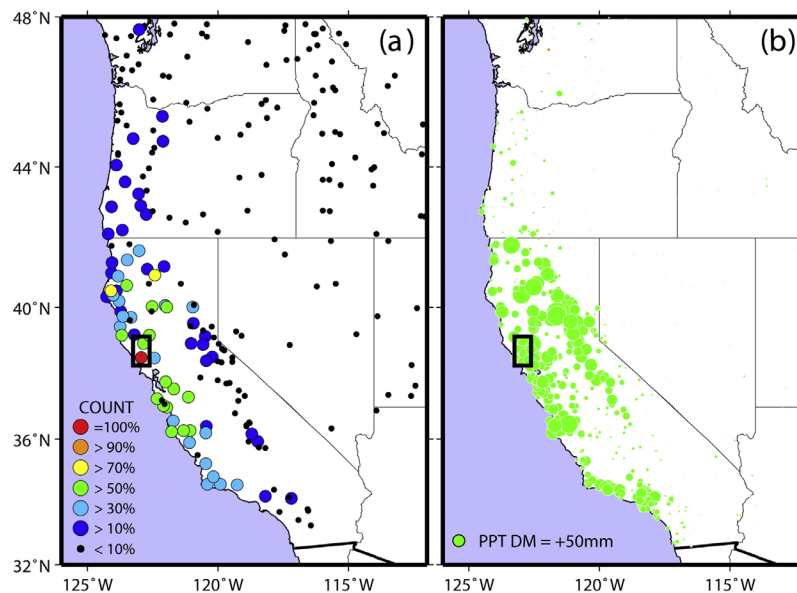


**Figure 6.** Statistical analyses based on the 7 flood- and monitor-stage events on California's Russian River at Guerneville (Table 1): (a) Percentage among the 7 events with daily streamflows in the top 0.8 percentile recorded by gauges spanning  $\geq 30$  years (see inset key); (b) departure from daily mean precipitation (sized for scale). The streamflow data are based on dates in local time coordinates ending at 11:59 p.m., whereas the daily precipitation data correspond to a 24-h period ending mid-morning local time (which may vary from site to site). The inset boxes mark the Russian River basin.

The analyses in Figure 6 illustrate the fact that the results for the Russian River likely also apply to a region roughly 500 km along the coast, although the highest amplitude response is limited to a more tightly-confined region.

## 5. Conclusions

[14] Observations from an 8-year-long series of field observations near the flood-prone Russian River of northern California were combined with SSM/I satellite observations offshore to explore the possible role of atmospheric rivers in creating the precipitation that led to flooding events on the Russian River. The contribution of atmospheric river conditions to the production of heavy orographic rainfall and ultimately to the flood of 16–18 February 2004 was documented most fully. To summarize, the spatial pattern of satellite-observed IWV conforms to the criteria used by *Ralph et al.* [2004] to characterize atmospheric rivers offshore; the GPS IWV observations at BBY exceeded 2 cm during the precipitation; and the wind profiler confirmed that the event occurred primarily within the warm sector of the storm and that LLJ conditions with strong upslope flow were prevalent. While the single case study provides a solid example of this relationship, all 7 flooding events on the Russian River at Guerneville since the suitable satellite and wind profiler data became available also were examined, and it was found that atmospheric river conditions were present and caused heavy rainfall through orographic precipitation for all 7 events. The regional extent of the heavy precipitation, warm temperatures, and flooding illustrated the regional impact of atmospheric rivers and the representativeness of the Russian River events. It should be recognized, however, that not all atmospheric rivers are flood producers, since individual atmospheric rivers may not generate sufficiently intense rainrates or because they may propagate too quickly across a given watershed. Additionally, if an atmospheric river is preceded by relatively dry conditions, the soil will have a much greater capacity to absorb heavy rainfall, thereby mitigating the potential for heavy runoff and flooding. In other words, while the presence of an atmospheric river was a necessary condition in all of the floods on the Russian River during this period, it was not a sufficient condition. Future work includes determining the predictability of this phenomenon (such as, distinguishing the characteristics of “null” cases where atmospheric rivers do not produce floods), and evaluation of the current forecast system with respect to the detection and prediction of atmospheric rivers, and their

overall role in the climatology of western U.S. precipitation [e.g., *Dettinger et al.*, 2004].

## References

- Andrews, E. D., R. C. Antweiler, P. J. Neiman, and F. M. Ralph (2004), Influence of ENSO on flood frequency along the California coast, *J. Clim.*, *17*, 337–348.
- Bao, J.-W., S. A. Michelson, P. J. Neiman, F. M. Ralph, and J. M. Wilczak (2006), Interpretation of enhanced integrated water-vapor bands associated with extratropical cyclones: Their formation and connection to tropical moisture, *Mon. Weather Rev.*, *134*(4), 1063–1080.
- Browning, K. A., and C. W. Pardoe (1973), Structure of low-level jet streams ahead of mid-latitude cold fronts, *Q. J. R. Meteorol. Soc.*, *99*, 619–638.
- Carter, D. A., K. S. Gage, W. L. Ecklund, W. M. Angevine, P. E. Johnston, A. C. Riddle, J. S. Wilson, and C. R. Williams (1995), Developments in UHF lower tropospheric wind profiling at NOAA's Aeronomy Laboratory, *Radio Sci.*, *30*, 997–1001.
- Dettinger, M., K. Redmond, and D. Cayan (2004), Winter orographic precipitation ratios in the Sierra Nevada—Large-scale atmospheric circulations and hydrologic consequences, *J. Hydrometeorol.*, *5*, 1102–1116.
- Higgins, R. W., J.-K. E. Schemm, W. Shi, and A. Leetmaa (2000), Extreme precipitation events in the western United States related to tropical forcing, *J. Clim.*, *13*, 793–820.
- Hollinger, J. P., J. L. Peirce, and G. A. Poe (1990), SSM/I instrument evaluation, *IEEE Trans. Geosci. Remote Sens.*, *28*, 781–790.
- Neiman, P. J., F. M. Ralph, A. B. White, D. E. Kingsmill, and P. O. G. Persson (2002), The statistical relationship between upslope flow and rainfall in California's coastal mountains: Observations during CALJET, *Mon. Weather Rev.*, *130*, 1468–1492.
- Ralph, F. M., P. J. Neiman, D. E. Kingsmill, P. O. G. Persson, A. B. White, E. T. Strem, E. D. Andrews, and R. C. Antweiler (2003), The impact of a prominent rain shadow on flooding in California's Santa Cruz Mountains: A CALJET case study and sensitivity to the ENSO cycle, *J. Hydrometeorol.*, *4*, 1243–1264.
- Ralph, F. M., P. J. Neiman, and G. A. Wick (2004), Satellite and CALJET aircraft observations of atmospheric rivers over the eastern North-Pacific Ocean during the winter of 1997/98, *Mon. Weather Rev.*, *132*, 1721–1745.
- Ralph, F. M., P. J. Neiman, and R. Rotunno (2005), Dropsonde observations in low-level jets over the Northeastern Pacific Ocean from CALJET-1998 and PACJET-2001: Mean vertical-profile and atmospheric-river characteristics, *Mon. Weather Rev.*, *133*, 889–910.
- Weaver, R. L. (1962), Meteorology of hydrologically critical storms in California, *Hydrol. Rep.* *37*, 207 pp., Hydrol. Serv. Div., U.S. Weather Bur., Washington, D. C.
- Wolfe, D. E., and S. I. Gutman (2000), Developing an operational, surface-based, GPS, water-vapor observing system for NOAA: Network design and results, *J. Atmos. Oceanic Technol.*, *17*, 426–440.
- Zhu, Y., and R. E. Newell (1998), A proposed algorithm for moisture fluxes from atmospheric rivers, *Mon. Weather Rev.*, *126*, 725–735.
- D. R. Cayan and M. D. Dettinger, U.S. Geological Survey, Scripps Institution of Oceanography, La Jolla, CA 92037, USA.
- S. I. Gutman, P. J. Neiman, F. M. Ralph, and G. A. Wick, NOAA/Earth System Research Laboratory, Boulder, CO 80305, USA. (marty.ralph@noaa.gov)
- A. B. White, Cooperative Institute for Research in the Environmental Sciences/NOAA/ESRL, Boulder, CO 80309, USA.